


# The unusual planetary nebula nucleus in the Galactic open cluster M37 and six further hot white dwarf candidates

Klaus Werner<sup>1</sup> , Nicole Reindl<sup>2,3</sup>, Roberto Raddi<sup>4</sup>, Massimo Griggio<sup>5,6</sup>, Luigi R. Bedin<sup>7</sup>, María E. Camisassa<sup>4</sup>, Alberto Rebassa-Mansergas<sup>4,7</sup>, Santiago Torres<sup>4,7</sup>, and Peter Goodhew<sup>8</sup>

<sup>1</sup> Institut für Astronomie und Astrophysik, Kepler Center for Astro and Particle Physics, Eberhard Karls Universität, Sand 1, 72076 Tübingen, Germany

e-mail: [werner@astro.uni-tuebingen.de](mailto:werner@astro.uni-tuebingen.de)

<sup>2</sup> Landessternwarte Heidelberg, Zentrum für Astronomie, Ruprecht-Karls-Universität, Königstuhl 12, 69117 Heidelberg, Germany

<sup>3</sup> Institut für Physik und Astronomie, Universität Potsdam, Karl-Liebknecht-Straße 24/25, 14476 Potsdam, Germany

<sup>4</sup> Departament de Física, Universitat Politècnica de Catalunya, c/Estève Terrades 5, 08860 Castelldefels, Spain

<sup>5</sup> Dipartimento di Fisica, Università di Ferrara, Via Giuseppe Saragat 1, Ferrara 44122, Italy

<sup>6</sup> INAF – Osservatorio Astronomico di Padova, Vicolo dell’Osservatorio 5, Padova 35122, Italy

<sup>7</sup> Institute for Space Studies of Catalonia, c/Gran Capità 2–4, Edif. Nexus 104, 08034 Barcelona, Spain

<sup>8</sup> W4 3EQ London, UK

Received 16 June 2023 / Accepted 15 September 2023

## ABSTRACT

Planetary nebulae in Galactic open star clusters are rare objects; only three are known to date. They are of particular interest because their distance can be determined with high accuracy, allowing one to characterize the physical properties of the planetary nebula and its ionizing central star with high confidence. Here we present the first quantitative spectroscopic analysis of a central star in an open cluster, namely the faint nucleus of IPHASX J055226.2+323724 in M37. This cluster contains 14 confirmed white dwarf members, which were previously used to study the initial-to-final-mass relation of white dwarfs, and six additional white dwarf candidates. We performed an atmosphere modeling of spectra taken with the 10m Gran Telescopio Canarias. The central star is a hot hydrogen-deficient white dwarf with an effective temperature of 90 000 K and spectral type PG1159 (helium- and carbon-rich). We know it is about to transform into a helium-rich DO white dwarf because the relatively low atmospheric carbon abundance indicates ongoing gravitational settling of heavy elements. The star belongs to a group of hot white dwarfs that exhibit ultrahigh-excitation spectral lines possibly emerging from shock-heated material in a magnetosphere. We find a relatively high stellar mass of  $M = 0.85^{+0.13}_{-0.14} M_{\odot}$ . This young white dwarf is important for the semi-empirical initial-final mass relation because any uncertainty related to white-dwarf cooling theory is insignificant with respect to the pre-white-dwarf timescale. Its post-asymptotic-giant-branch age of 170 000–480 000 yr suggests that the extended planetary nebula is extraordinarily old. We also performed a spectroscopic analysis of the six other white dwarf candidates of M37, confirming one as a cluster member.

**Key words.** open clusters and associations: individual: M37 – planetary nebulae: individual: IPHASX J055226.2+323724 – stars: atmospheres – stars: evolution – white dwarfs

## 1. Introduction

In a recent astro-photometric study of the Galactic open cluster M37 (NGC 2099), [Griggio et al. \(2022\)](#) identified seven hot white dwarfs as cluster member candidates. One of these white dwarfs (labeled WD1 in their list) is a high-probability cluster member as well as the probable central star of a planetary nebula (PN; [Chornay & Walton 2020](#)). The large, evolved, and bipolar PN IPHASX J055226.2+323724 (or PN G177.5+03) was confirmed to be a member of M37 ([Fragkou et al. 2022b](#)). It is only the third known PN in a Galactic open cluster, the other two being the PNe in NGC 6067 and Andrews-Lindsay 1 ([Fragkou et al. 2022a, 2019; Parker et al. 2011](#)).

The central star WD1 (*Gaia* DR3 3451205783698632704, RA 05<sup>h</sup>52<sup>m</sup>26<sup>s</sup>.19, Dec. +32° 37′ 24″.89, J2000) in M37 is a faint ( $V = 19.16$ ) blue star located at the geometrical center of the PN ([Fragkou et al. 2022b](#)). Low-resolution spectroscopy presented by [Griggio et al. \(2022\)](#) shows it to be a hydrogen-deficient white dwarf with a spectral type between DO and PG1159 and an effective temperature above  $T_{\text{eff}} = 60\,000$  K.

The open cluster M37 has long been known to contain a large white dwarf population of at least 14 confirmed members ([Kalirai et al. 2005; Cummings et al. 2015](#)), including a very massive one ( $1.28 M_{\odot}$ ) whose progenitor evolution is uncertain ([Cummings et al. 2016](#)). Due to this richness of white dwarf members, M37 has been the focus of detailed studies on the initial-to-final-mass relation (IFMR) of white dwarfs that connects their masses to those of their progenitors ([Cummings et al. 2015, 2018](#)).

Here, we present new spectroscopic observations of WD1 and a non-local thermodynamic equilibrium (non-LTE) model atmosphere analysis as well as new deep imaging of the PN. In addition, we performed spectroscopic observations and analyses of the six other hot DA white dwarf member candidates of M37 identified by [Griggio et al. \(2022\)](#) in order to further investigate their possible membership. In Sect. 2, we introduce our observations. We continue in Sect. 3 with the spectral analysis of the white dwarfs, focusing on the PN nucleus WD1. In Sect. 4, we perform fits to the spectral energy distribution (SED) of the white dwarfs and present the results. We finish in Sect. 5 with a

**Table 1.** Logs of the GTC observations.

Name ID	Short name	<i>Gaia</i> <i>G</i> (mag)	Grism	Resolution (Å)	Date	Seeing (arcsec)	Exposure (s)
WD1	0552+3237	19.154	R2000B	3.0	20220921	0.8	4 × 750
					20220923		4 × 750
WD2	0552+3236	20.137	R1000B	9.0	20221003	1.1	2 × 1400
WD3	0552+3231	19.769	R1000B	9.0	20220929	1.1	2 × 1400
WD4	0551+3216	20.560	R1000B	9.0	20221016	0.7	4 × 1000
WD5	0553+3229	20.660	R1000B	9.0	20220929	1.2	2 × 1000
					20221017		2 × 1000
WD6	0547+3246	19.917	R1000B	9.0	20221003	0.7	2 × 1400
WD7	0548+3323	20.599	R1000B	9.0	20220929	1.3	2 × 1000
					20221016		2 × 1000

summary of our study as well as a discussion on the contribution of the confirmed members to the IFMR of white dwarfs in open clusters.

## 2. Observations

### 2.1. Spectroscopy

We acquired low-resolution long-slit optical spectra for all seven white dwarf candidates in M37 that were identified by Griggio and collaborators. These observations were performed in service mode at the 10m Gran Telescopio Canarias (GTC) in gray and dark time, in September and October 2022 (proposal ID: GTC72-22B). We obtained 4 × 750 s exposures for WD1, both with the R2000B and R2500R gratings, employing a 1-arcsecond slit, and standard 2 × 2 binning and slow readout. The resolving power at the central wavelengths of both spectral regions is  $R \sim 1500$ . The other targets were observed with the R1000B grating, delivering a resolving power of  $R \sim 800$ , with exposure times ranging between 1000–1400 s and obtaining between 2 and 4 exposures per star, depending on their apparent magnitudes. The average seeing was below 1.3 arcsec with no cloud coverage. All targets were observed at an airmass smaller than 1.3. The observing log is listed in Table 1.

We performed pre-reduction data manipulation, bias and flat-field correction, and optical extraction of the long-slit spectra (Horne 1986) by using the STARLINK (Berry et al. 2022) and PAMELA software (Marsh 1989). The wavelength and flux calibration used the nightly observations of HgAr and Ne lamps and the flux standards, respectively; finally, each sub-exposure was co-added, achieving a signal-to-noise ratio  $S/N \gtrsim 20$  at the H $\alpha$  wavelength. These tasks were performed using the MOLLY software (Marsh 1989). The rectified spectrum of WD1 is shown in Fig. 1.

### 2.2. Imaging

The PN IPHASXJ055226.2+323724 was discovered by Sabin (2008) on images from the IPHAS survey (Drew et al. 2005; see in particular the image versions presented by Fragkou et al. 2022b and Griggio et al. 2022). The PN has a bipolar structure with a major axis of about 7.5 arcmin and a patchy internal structure.

We present in Fig. 2 our new image, which reveals more details of the PN structure. The data for the image were recorded on August 30 and September 10, 2022, using two remote robotic

observatories located at the e-EyE telescope hosting site<sup>1</sup> near Fregenal de la Sierra in southwestern Spain. The one observatory was equipped with twin APM TMB LZOS 152 refractors<sup>2</sup> and QSI 6120wsg CCD cameras<sup>3</sup>. Broadband filters used were Astrodon<sup>4</sup> red, green, and blue. Narrowband filters were Astrodon O III  $\lambda 5007$  Å with 30 Å bandpass and Astrodon H $\alpha$  with 50 Å bandpass. The other observatory was equipped with a Celestron EdgeHD 14-inch reflector<sup>5</sup> and a ZWO ASI6200MM Pro CCD camera<sup>6</sup>. Employed filters were Chroma<sup>7</sup> O III  $\lambda 5007$  Å and H $\alpha$  both with 30 Å bandpass. The total O III and H $\alpha$  data integrations were 48:10 and 27:45 h, respectively. The total integration time for broadband blue and green was 2:45 h each and 2:55 h for red. Image preprocessing and stacking was performed using PIXINSIGHT<sup>8</sup> and image processing using PIXINSIGHT and PHOTOSHOP<sup>9</sup>.

## 3. Spectral analysis

### 3.1. WD1, the central star of IPHASXJ055226.2+323724

The spectrum of WD1 is dominated by the hallmark of PG1159 stars, a broad absorption trough formed by He II 4686 Å and a few C IV lines around 4650 Å (Fig. 1). PG1159 stars are hydrogen-deficient objects that have suffered a late helium-shell flash (see, e.g., Werner & Herwig 2006). WD1 belongs to the spectral subtype “A” (Werner 1992), indicating that the lines in the trough are in pure absorption and that the effective temperature is around 90 000 K. The strong decrement of the He II Pickering line series points at a surface gravity larger than  $\log g = 7$ . In addition, a few other very weak C IV lines are detected. We also identify four non-photospheric, ultrahigh-excitation (UHE) lines from C V, C VI, O VII, and O VIII. These lines require extremely high temperatures in their formation region (on the order of  $10^6$  K, Werner et al. 1995). About 10% of the hottest white dwarfs show this UHE phenomenon, and it was suggested that the UHE lines form in a circumstellar magnetosphere (Reindl et al. 2019, 2021).

<sup>1</sup> <https://www.e-eye.es/en/hosting/>

<sup>2</sup> <https://www.apm-telescopes.net/en>

<sup>3</sup> <https://qsimaging.com/>

<sup>4</sup> <https://farpointastro.com/collections/astrodon>

<sup>5</sup> <https://www.celestron.com/>

<sup>6</sup> <https://astronomy-imaging-camera.com/>

<sup>7</sup> <https://www.chroma.com/>

<sup>8</sup> <https://pixinsight.com/>

<sup>9</sup> <https://www.adobe.com/de/products/photoshopfamily.html>

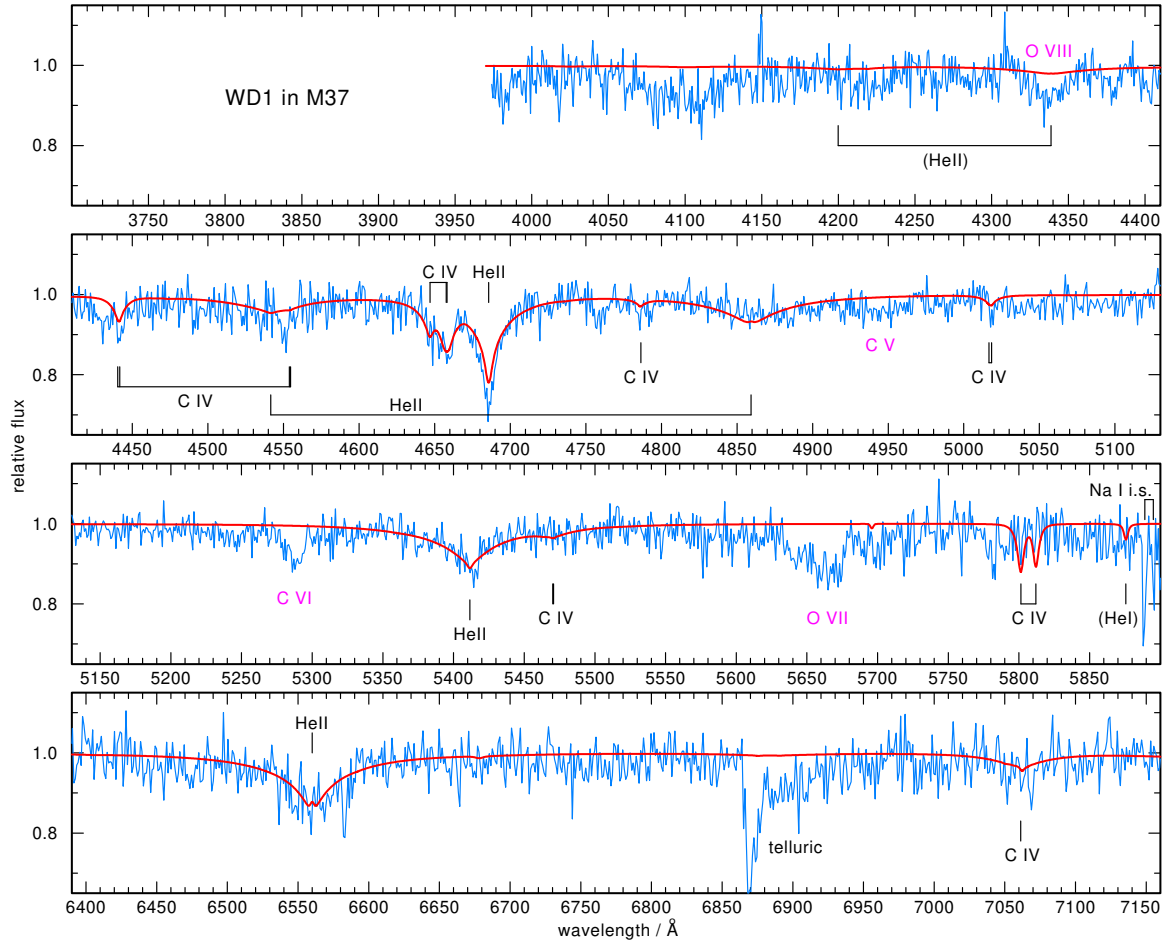


**Fig. 1.** GTC spectrum of WD1, the hydrogen-deficient central star of the PN IPHASX J055226.2+323724, and our final model (red graph) with  $T_{\text{eff}} = 90\,000$  K,  $\log g = 8.3$ , He = 0.94, and C = 0.06 (mass fractions). Identified lines are labeled. Non-photospheric UHE lines of C V-VI and O VII-VIII have violet labels.



**Fig. 2.** PN IPHASX J055226.2+323724 in the open cluster M37. *Left:* co-addition of all observations, with a total exposure time of 3.52 days as described in the text.  $H\alpha$  is mapped to red and [O III] 5007 Å to green. Broadband frames of the stellar field are mapped to red, green, and blue. The height of the frame is 25'. North is up and east to the left. Note the faint nebulosity at the southeastern rim of the cluster. *Right:* zoomed-in view of the left panel, with the PN central star circled in green.

For the spectral analysis of WD1 we computed a small grid of non-LTE model atmospheres of the type introduced by Werner et al. (2014). It was calculated using the Tübingen Model-Atmosphere Package (TMAP) for non-LTE plane-parallel models in radiative and hydrostatic equilibrium (Werner et al. 2003). The constituents of the models are helium and carbon. The grid

covers the range  $T_{\text{eff}} = 70\,000\text{--}110\,000$  K in steps of 10 000 K, and  $\log g = 7.5\text{--}8.5$  in steps down to 0.2 dex. At the outset the mass fractions of helium and carbon were fixed to He = 0.91 and C = 0.09. This is a low carbon abundance for a PG1159 star and it was chosen because of the relative weakness of the C IV lines compared to many other stars of the PG1159 class. In the course

**Table 2.** Atmospheric properties and other parameters of the white dwarf central star WD1 in M37.

Parameter	Value
Spectral type	PG1159
$T_{\text{eff}}$ (K)	$90\,000 \pm 10\,000$
$\log(g)$ ( $\text{cm s}^{-2}$ )	$8.3 \pm 0.3$
He	$0.94 \pm 0.03$
C	$0.06 \pm 0.03$
$L$ ( $L_{\odot}$ )	$13_{-11}^{+20}$
$R$ ( $R_{\odot}$ )	$0.015_{-0.005}^{+0.011}$
$M$ ( $M_{\odot}$ ) (VLTP)	$0.85_{-0.14}^{+0.13}$
$d$ (pc) (SED fit)	$800_{-250}^{+380}$
$d$ (pc) ( <i>Gaia</i> parallax)	$1272_{-418}^{+905}$
$d$ (pc) (M37)	$1490 \pm 90$

**Notes.** Element abundances given in mass fractions. Stellar mass derived from VLTP tracks (Fig. 3). The *Gaia* distance of WD1 is taken from Bailer-Jones et al. (2021) and the distance of M37 from Griggio & Bedin (2022) using *Gaia* Early Data Release 3 data.

of the analysis, the carbon abundance in some models was varied to find the finally adopted value and to estimate errors. It should be noted that we do not attempt to model the non-photospheric UHE lines.

The best-fit model was determined by the following procedure. The He II 4860 Å line is virtually absent in the observation and it was found that within the considered temperature range only models with sufficiently high surface gravity (around  $\log g = 8.5$ ) can match the observation. A lower limit to the temperature is provided by the absence of He I 5876 Å in the observation, meaning that  $T_{\text{eff}}$  is at least 80 000 K. An upper limit of 100 000 K was estimated, because at higher values He II 4686 Å becomes very weak and the He II Pickering lines at 5410 and 6560 Å develop emission cores that are not observed. By visual inspection of the helium lines we finally adopted  $T_{\text{eff}} = 90\,000 \pm 10\,000$  K and  $\log g = 8.3 \pm 0.3$ . The carbon abundance is  $C = 0.06 \pm 0.03$  by mass. The final model spectrum is depicted in Fig. 1. The atmospheric parameters of WD1 together with other characteristics are summarized in Table 2.

It can be seen that the computed He II 4686 Å line is not deep enough. This could be related to the He II line problem observed in other UHE stars (Reindl et al. 2021). This means that the He II lines are too deep to be fitted by any model. On the other hand, this problem also affects other lines besides He II 4686 Å, but in the case of WD1 the 5410 and 6560 Å lines are reproduced very well by our model. The C IV 5801/5812 Å doublet in the synthetic spectrum is not visible in the observation. It could be that the S/N of the spectrum is not sufficient to resolve the two lines because they are narrower than the He II lines. This doublet is known to turn from absorption into emission at a temperature of about 100 000 K (Werner 1992). Therefore, a model at the upper limit of our  $T_{\text{eff}}$  estimate is in accordance with the non-detection in the observation. But we note that at 100 000 K the He II 4686 Å line is significantly weaker and hence gives a poorer fit than our final model with  $T_{\text{eff}} = 90\,000$  K.

Figure 3 shows the location of WD1 in the Kiel ( $\log g$ – $\log T_{\text{eff}}$ ) diagram together with all other objects of the PG1159 class<sup>10</sup> and the helium-dominated DO white dwarfs and O(He)

stars. WD1 is remarkable because it is the PG1159 star with the highest surface gravity. Comparison with the depicted evolutionary tracks gives a mass of  $M = 0.85_{-0.14}^{+0.13} M_{\odot}$ , making WD1 the second of the two most massive members of its spectral class.

The initial main-sequence progenitor mass  $M_{\text{init}}$  of a white dwarf in a stellar cluster can be determined from isochrones that are inferred from stellar evolution models. One creates an isochrone at the progenitor’s evolutionary lifetime and metallicity. The isochrone’s given  $M_{\text{init}}$  of a star at the tip of the asymptotic giant branch (AGB) is the white dwarf’s  $M_{\text{init}}$ . To be consistent with the results of the work of Cummings et al. (2018) for other white dwarf members of M37, we adopt a cluster age of  $585 \pm 50$  Myr and the following procedure to construct PARSEC isochrones (Bressan et al. 2012). We used the web interface CMD3.7<sup>11</sup> and chose PARSEC version 1.2S and a solar metallicity ( $Z = 0.0152$ ). The resulting isochrones end at the tip of the AGB. Since the cooling age of WD1 (some  $10^5$  yr; see below) is completely negligible compared to the cluster age, its initial mass is identical to the mass of current M37 stars at the tip of the AGB. We find  $M_{\text{init}} = 2.77_{-0.08}^{+0.09} M_{\odot}$ , in good agreement with Fragkou et al. (2022b). The error reflects the uncertainty of the cluster age.

Cummings et al. (2018) have determined initial and final masses of 14 white dwarfs in M37. They are displayed in Fig. 4 (we do not plot an outlier, the ultra-massive white dwarf termed WD33 in their paper) together with WD1, the central star of the PN, which is also the youngest cluster white dwarf. It is an important point in the IFMR because it is independent of any possible uncertainties in white-dwarf cooling theory. The initial and final masses of WD1 are consistent with the IFMR determined by Cummings et al. (2018) from eighty white dwarfs, shown by the blue graph in Fig. 4. All these white dwarfs are hydrogen-rich (spectral type DA) in contrast to WD1. However, there is no clear evidence that the IFMR for hydrogen-deficient white dwarfs is different (Barnett et al. 2021).

### 3.2. DA white dwarfs

Using a pure-hydrogen non-LTE model grid computed with TMAP (Reindl et al. 2023), we derived effective temperatures and surface gravities for the three hottest DA white dwarfs. This was done by fitting the observed Balmer lines by means of  $\chi^2$  minimization using the FITSB2 routine (Napiwotzki 1999) and calculating the statistical  $1\sigma$  errors. For WD3 (WD0552+3231) we excluded the H  $\delta$  line from the fit as it was affected by a cosmic ray hit. We derive  $T_{\text{eff}} = 94\,220 \pm 14\,702$  K and  $\log g = 6.91 \pm 0.16$ . For WD2 (WD0552+3236) we find  $T_{\text{eff}} = 76\,043 \pm 4640$  K and  $\log g = 8.08 \pm 0.29$ , and for WD6 (WD0547+3246) we determine  $T_{\text{eff}} = 48\,690 \pm 1430$  K and  $\log g = 7.72 \pm 0.16$ .

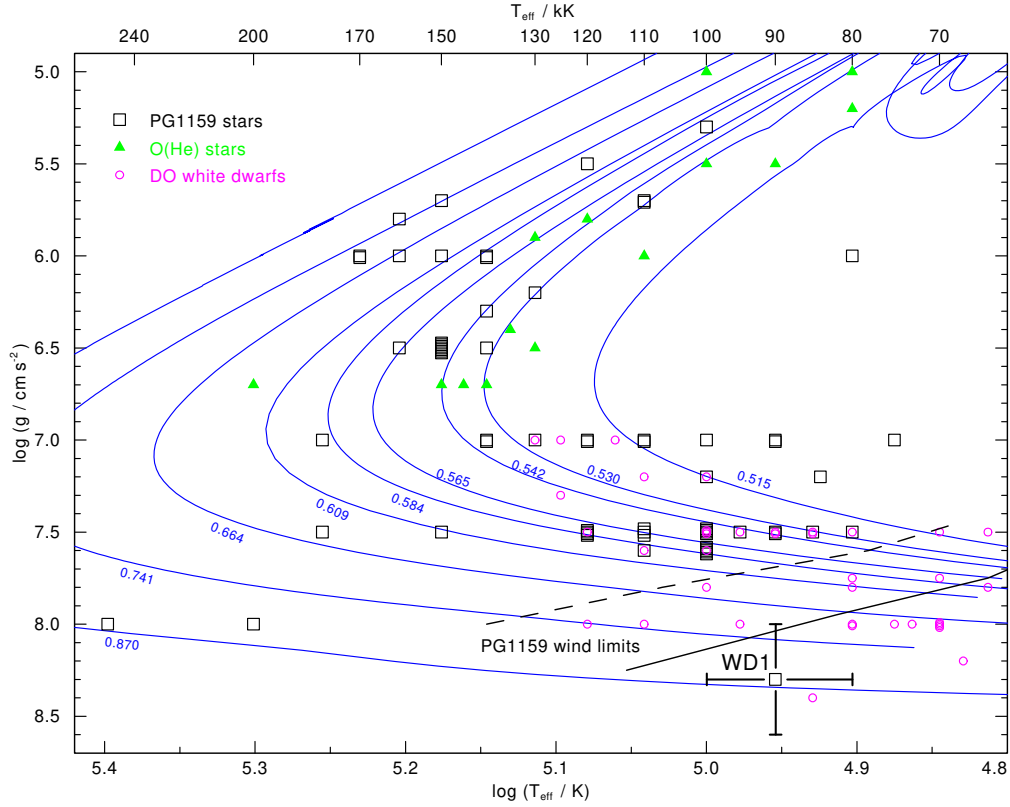
The three coolest white dwarfs were analyzed with a grid of hydrogen-dominated synthetic spectra (Koester 2010). We employed FITSB2 for fitting six Balmer lines per star. The best-fit results are shown in Fig. 5 for both the hot and cool white dwarfs. The atmospheric parameters ( $T_{\text{eff}}$  and  $\log g$ ) are listed in Table 3.

## 4. SED fitting

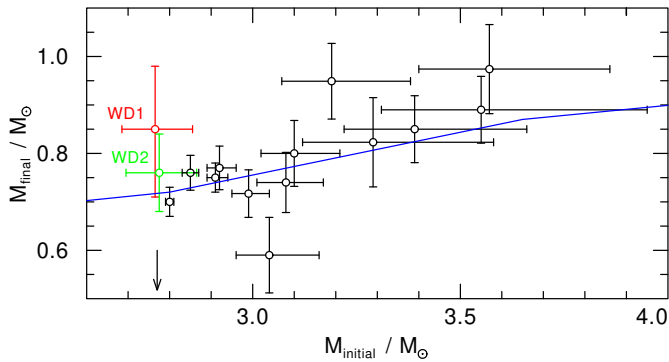
Subsequently, we collected available photometry from the Galaxy Evolution Explorer (GALEX; DR6+7; Bianchi et al. 2017), IGAPS (Monguió et al. 2020), Pan-STARRS

<sup>10</sup> According to an unpublished list based on Werner & Herwig (2006) and maintained by one of the authors (KW).

<sup>11</sup> [http://stev.oapd.inaf.it/cgi-bin/cmd\\_3.7](http://stev.oapd.inaf.it/cgi-bin/cmd_3.7)

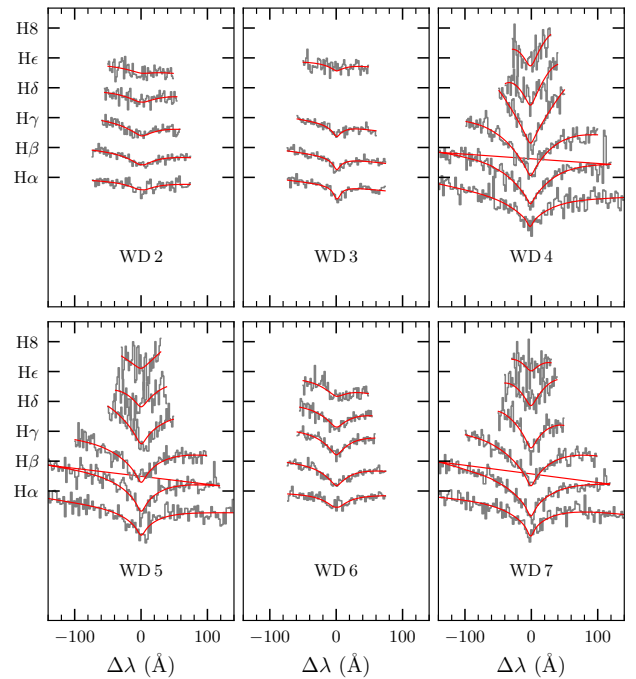


**Fig. 3.** Position and error bars of the PG1159 star WD1 in the Kiel diagram together with all known objects of this spectral class. Also shown are the positions of other hot helium-dominated objects, namely DO white dwarfs and O(He) stars. Evolutionary tracks by Althaus et al. (2009) are labeled with the stellar mass in solar units. The black line indicates the PG1159 wind limit according to Unglaub & Bues (2000), meaning that the mass-loss rate of the radiation-driven wind at this position of the evolutionary tracks becomes so weak that gravitational settling of heavy elements is able to remove the heavy elements from the white dwarf atmosphere. Thus, no PG1159 stars should be found at significantly cooler temperatures. The dashed line is the wind limit assuming a mass-loss rate that is ten times lower. The fact that many PG1159 stars and DO white dwarfs are located at (half-)integer  $\log g$  values is an artifact due to the spacing of model atmosphere grids employed for spectral analyses.



**Fig. 4.** IFMR relation for white dwarfs in the open cluster M37. The red symbol indicates the PN central star WD1 and the green symbol WD2 from our study. The other white dwarfs are from Cummings et al. (2018). The blue graph, taken from that paper, is the semi-empirical three-piece linear fit to white dwarfs in several open clusters based on PARSEC isochrones. The vertical arrow points to the current M37 progenitor mass at the tip of the AGB.

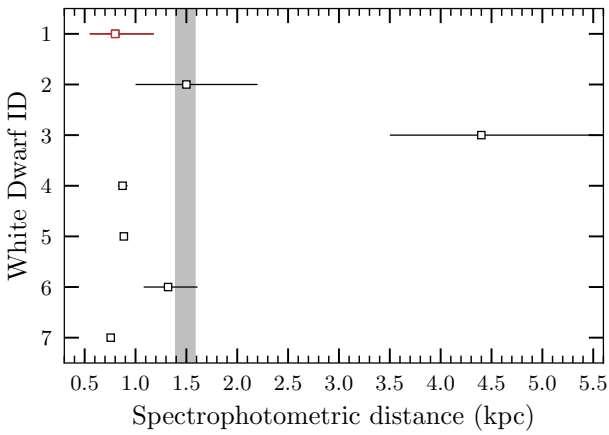
(Chambers et al. 2016), *Gaia* (Gaia Collaboration 2021), the XMM-OM Serendipitous Source Survey Catalogue (Page et al. 2012), and the Sloan Digital Sky Survey (SDSS; DR12; Alam et al. 2015), in order to estimate the spectrophotometric distances of WD1 and the six DA white dwarfs via fits of their SEDs. The  $T_{\text{eff}}$  and  $\log g$  are fixed priors, while the white dwarf radii



**Fig. 5.** Best-fit results of the spectral analysis for the six DA white dwarfs. The observed Balmer lines and the best-fit models are shown in gray and red, respectively. The respective values for  $T_{\text{eff}}$  and  $\log g$  are given in Table 3.

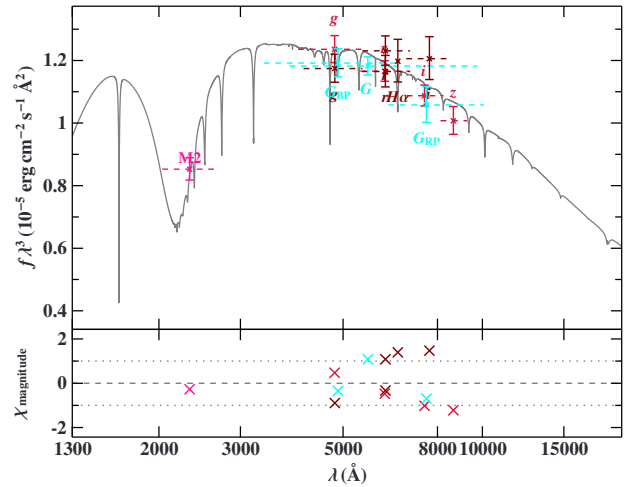
**Table 3.** Atmospheric and physical parameters of the six DA white dwarfs determined via spectroscopic and photometric analysis.

Name ID	Short name	<i>Gaia</i> ID	$T_{\text{eff}}$ (K)	$\log g$ (cgs)	Mass ( $M_{\odot}$ )	$\tau_{\text{cool}}$ (Myr)	$d$ (kpc)
WD 2	0552+3236	3451182182857026048	$76\,000 \pm 4640$	$8.08 \pm 0.29$	$0.76 \pm 0.08$	$0.51^{+0.11}_{-0.21}$	$1.5^{+0.7}_{-0.5}$
WD 3	0552+3231	3451201076423973120	$94\,220 \pm 14\,700$	$6.91 \pm 0.16$	$0.52 \pm 0.07$	$0.02^{+0.10}_{-0.01}$	$4.4^{+1.1}_{-0.9}$
WD 4	0551+3216	3451167786125150592	$19\,080 \pm 1580$	$7.76 \pm 0.27$	$0.51 \pm 0.11$	$112^{+113}_{-45}$	$0.87 \pm 0.05$
WD 5	0553+3229	3451200114340263296	$29\,630 \pm 1030$	$8.08 \pm 0.31$	$0.68 \pm 0.11$	$11^{+22}_{-2}$	$0.90 \pm 0.04$
WD 6	0547+3246	3448258267902375296	$48\,690 \pm 1430$	$7.72 \pm 0.16$	$0.57 \pm 0.06$	$2.4^{+0.3}_{-0.5}$	$1.32^{+0.29}_{-0.24}$
WD 7	0548+3323	3454340495645123584	$25\,420 \pm 1580$	$8.04 \pm 0.28$	$0.65 \pm 0.12$	$24^{+47}_{-6}$	$0.76 \pm 0.03$


**Fig. 6.** Spectrophotometric distances for the six DA white dwarfs and the central star WD1 (red symbol) compared with the *Gaia*-based distance of M37 obtained by Griggio et al. (2022).

and masses are determined via interpolation from evolutionary tracks. For the DA white dwarfs we employed tracks for He-core and CO-core white dwarfs from Hall et al. (2013) and Renedo et al. (2010), respectively. For WD1 we employed very late thermal pulse (VLTP) tracks from Althaus et al. (2009). Thus, their distances are estimated through minimization of the  $\chi^2$  between observed and synthetic SED, by assuming the radius to be fixed within the measured uncertainties while distance and interstellar extinction are free parameters. The Fitzpatrick et al. (2019) extinction law for  $R_V = 3.1$  is adopted. For the six DA white dwarfs the results are given in Table 3. For WD1 we additionally calculated the radius from the angular diameter (as derived from the SED fit) and the Bailer-Jones distance. Furthermore, we calculated the luminosity from the radius and the effective temperature via  $L/L_{\odot} = (R/R_{\odot})^2 (T_{\text{eff}}/T_{\text{eff},\odot})^4$ . The results for WD1 are listed in Table 2. In Fig. 6 the spectrophotometric distances of WD1–WD7 are compared to the *Gaia*-based distance of M37 obtained by Griggio et al. (2022). Their method of SED fitting is the same as ours, so we refrain from showing the SED fits for WD2–WD7. The SED fit for WD1 is shown in Fig. 7.

One possible explanation for the short spectrophotometric distance determined for WD1 compared with the distance of M37 could be that the optical flux of the model is underestimated because it neglects opacities of all metals except of carbon. They would block the radiation flux in the ultraviolet, which is redistributed into the optical wavelength range. To quantify this effect is difficult because the metal abundances can be assessed only from UV spectra. As an example we can look at the DO white


**Fig. 7.** SED fit for WD1. Filter-averaged fluxes converted from observed magnitudes are shown in different colors (*Gaia* in cyan, IGAPS in dark red, Pan-STARRS in red, and XMM-OM in magenta). The respective full widths at tenth maximum are shown as dashed horizontal lines. A pure He model with  $T_{\text{eff}} = 90\,000$  K and  $\log g = 8.3$  that was interpolated from the grid computed in Reindl et al. (2023) and degraded to a spectral resolution of  $6 \text{ \AA}$  is plotted in gray. To reduce the steep SED slope, the flux has been multiplied by the wavelength cubed. Bottom panel: Difference between synthetic and observed magnitudes.

dwarf HE 0504–2408. Its atmospheric parameters are similar to WD1:  $T_{\text{eff}} = 85\,000$  K,  $\log g = 7$ . From a UV spectral analysis the metal abundances of eleven species were determined (Werner et al. 2018). Taking the respective model atmosphere and comparing it to a metal-free model shows that the flux increase in the optical by UV metal-line blanketing amounts to 10%. That would transfer to a distance greater by only 5% unless the metal abundances are significantly higher.

## 5. Summary and discussion

We have performed a spectroscopic analysis of the central star of the PN IPHASX J055226.2+323724 in the Galactic open cluster M37. The object, WD1, is a hot hydrogen-deficient white dwarf composed of He =  $0.94 \pm 0.03$  and C =  $0.06 \pm 0.03$  (mass fractions). Its effective temperature of  $90\,000 \pm 10\,000$  K and high surface gravity of  $\log g = 8.3 \pm 0.3$  in comparison with evolutionary tracks for H-deficient stars (Althaus et al. 2009) yield a high mass of  $M = 0.85^{+0.13}_{-0.14} M_{\odot}$ . This is significantly higher than the mean mass of white dwarfs ( $0.61 M_{\odot}$ ; Kepler et al. 2016). It is also higher than the mass estimated by Fragkou et al. (2022b),

$0.63 M_{\odot}$ , from the PN kinematical age and the absolute V magnitude of the PN central star using evolutionary tracks from [Miller Bertolami \(2016\)](#). However, these tracks are for hydrogen-rich stars and therefore not appropriate for WD1.

The post-AGB (cooling) age of WD1 can be estimated from the evolutionary tracks depicted in [Fig. 3](#). At the location of WD1, the cooling age is linearly interpolated from the two neighboring tracks, and we determine  $\tau_{\text{cool}} = 350\,000$  yr. Considering the error bars in temperature and gravity, we find a range of 170\,000–480\,000 yr. This is significantly longer than the kinematic age of the PN,  $78\,000 \pm 25\,000$  yr, as estimated by [Fragkou et al. \(2022b\)](#). The reason for this discrepancy is unclear. They determined the kinematic age assuming a constant PN expansion rate, which might not be realistic. Alternatively, the evolutionary rate of the central star could be underestimated by the stellar models. It was shown recently by [Miller Bertolami \(2016\)](#) that new calculations with improved input physics can considerably speed up the post-AGB evolution compared to earlier models. However, new models for H-deficient post-AGB stars with masses relevant to WD1 are not available. In any case, because of the high initial mass of the main-sequence progenitor, the PN mass should be rather high,  $M \approx 1.9 M_{\odot}$ , which would favor a long PN visibility. Only a small fraction of this gas mass is ionized, namely  $M = 0.32 M_{\odot}$  ([Fragkou et al. 2022b](#)). Consequently, the real kinematic age of the PN could be even older. In this context we note that there is a faint nebulosity at the southeastern rim of the cluster in [Fig. 2](#) that is not visible in the IPHAS image presented in [Fragkou et al. \(2022b\)](#). Spectroscopy and kinematical data could reveal whether it is connected to the PN, although this appears rather unlikely because the PN would have to be exceptionally large and old.

Another fact that complicates the determination of the cooling age of WD1 is its hydrogen-deficient nature. PG1159 stars are assumed to be the result of a late He-shell flash experienced by a post-AGB star or white dwarf that brings the star back onto the AGB (the born-again star scenario; see, e.g., [Werner & Herwig 2006](#))<sup>12</sup>. Hence, the age derived from the tracks of [Althaus et al. \(2009\)](#) starts from the time when the star left the AGB for the second time. So if we assume that the PN was ejected at the first departure of the star from the AGB, then in principle the PN could be even older. This seems to be highly improbable. Therefore, one can conclude that the late He-shell flash in the precursor of WD1 occurred soon after or even just before the first departure from the AGB; otherwise, the PN would have been dispersed long ago. These are the particular cases of a late thermal pulse (LTP) or AGB final thermal pulse (AFTP) scenarios, respectively, in contrast to the VLTP case that a star suffers as a white dwarf. Evolutionary models predict relatively high amounts of surface hydrogen and nitrogen in the AFTP and LTP cases. So we expect spectral features of these elements in optical spectra of WD1, but their detection would require spectra with higher S/N and resolution.

A further indication that WD1 is a very evolved central star is its carbon abundance. We find  $C/He = 0.06$  (mass ratio). This is the lowest such value of any PG1159 star.  $C/He = 0.09$ – $1.5$  was determined in other members of this spectral class ([Werner & Herwig 2006](#)). Due to gravitational settling, carbon will sink out of the atmosphere as soon as the residual radiation-driven

wind of the star becomes too weak to be able to act against gravitational settling. This defines the so-called wind limit(s) indicated in the Kiel diagram in [Fig. 3](#). A PG1159 star will experience a reduction in carbon when it approaches the wind limit and will eventually transform into a pure-helium DO white dwarf. Wind limits were found from theoretical diffusion models, and their exact location in the Kiel diagram depends on the mass-loss rate assumed for the evolutionary models (which in turn depends, for example, on the metallicity). [Figure 3](#) shows two such wind limits taken from [Unglaub & Bues \(2000\)](#). WD1 is very close to these limits and, formally, is the only PG1159 star that has crossed these limits. Obviously, WD1 is in the final stage of PG1159 star evolution and is currently transforming into a DO white dwarf.

The spectrum of WD1 reveals the presence of UHE lines. About 10% of all hot white dwarfs ( $T_{\text{eff}} > 50\,000$  K) show this phenomenon. These lines were tentatively identified as Rydberg lines of UHE metals (e.g., O VIII) in ionization stages V–X ([Werner et al. 1995](#)). This would require a dense environment with temperatures near  $10^6$  K, and it has been proposed that the UHE lines form in a shock-heated, circumstellar magnetosphere ([Reindl et al. 2019](#)). Furthermore, UHE white dwarfs constitute a new class of variable stars ([Reindl et al. 2021](#)). Three-quarters of the 16 investigated UHE white dwarfs were found to exhibit a periodic variability with  $P = 0.22$ – $2.93$  days and amplitudes from a few tenths to a few hundredths of a magnitude. Spots on the surface of these stars and/or geometrical effects of circumstellar material might be responsible for this. Our WD1 central star was classified as a rotating variable with a period of 0.4451 day and an amplitude of 0.074 mag ([Chang et al. 2015](#); their designation for the star is V1975). Hence, WD1 belongs to this new class of variable UHE stars.

It is also noteworthy that the UHE phenomenon is, for an unknown reason, mainly exhibited by helium-rich white dwarfs (spectral types DO and DOZ; “Z” indicates the presence of metal lines, usually from carbon). Only three of the 17 known UHE stars are hydrogen-rich white dwarfs (spectral types DA and DAO; “O” indicates the presence of helium). Among the DOZ white dwarfs are two PG1159 stars (i.e., H-deficient objects with very high carbon abundance). WD1 is only the third PG1159 star known to exhibit UHE lines. The other two have temperatures similar to that of WD1. They are SDSS J121523.09+120300.8 with  $T_{\text{eff}} = 100\,000$  K and  $\log g = 7.6$  ([Hügelmeier et al. 2006](#)) and WD J070204.29+051420.56 with  $T_{\text{eff}} = 100\,000$  K and  $\log g = 7.5$  ([Reindl et al. 2023](#)).

We determined the main-sequence progenitor mass of WD1,  $M_{\text{init}} = 2.77^{+0.09}_{-0.08} M_{\odot}$ , from isochrones. WD1 is the youngest member in M37, younger than the 14 white dwarfs studied by [Cummings et al. \(2018\)](#). Its cooling time is negligible compared to the cluster age. Therefore, it is an important point in the IFMR because it is independent of any possible uncertainties in white-dwarf cooling theory. The initial and final masses of WD1 are consistent with the IFMR determined by [Cummings et al. \(2018\)](#), see our [Fig. 4](#).

Our study reveals that only two of the six DA white dwarfs (WD2 and WD6) have spectrophotometric distances consistent with that of M37 (see [Fig. 6](#) and [Table 4](#)). WD3 appears to be a background star, and the spectroscopic distances of the remaining three DAs suggest that they are foreground stars. Interestingly, [Griggio et al. \(2023\)](#) recently found that WD1, WD2, and WD3 should be cluster members according to their proper motions. WD3 is the hottest DA in our sample, and we note that the spectrum of this star was affected by a cosmic particle hit; thus, we had to exclude  $H\delta$  from our fit. In addition, it has to

<sup>12</sup> Recently, an alternative channel for the formation of PG1159 stars via a binary white dwarf merger was discussed with the discovery of so-called CO-sdO stars ([Werner et al. 2022](#)), but this should not produce PG1159 stars associated with a PN.

**Table 4.** Spectroscopic distance-, proper motion (PM)-, and single star evolution mass-based membership to M37 and progenitor parameters of our considered white dwarfs.

Name ID	$d_{\text{spec}}$	PM	$M \gtrsim 0.7 M_{\odot}$
WD 1	✗	✓	✓
WD 2	✓	✓	✓
WD 3	✗	✓	✗
WD 4	✗	?	✗
WD 5	✗	✗	✓
WD 6	✓	?	✗
WD 7	✗	?	✓

**Notes.** Proper-motion memberships have been taken from Griggio et al. (2023).

be stressed that atmospheric parameters of very hot DA white dwarfs derived from optical spectra can suffer large systematic errors (e.g., Werner et al. 2019). Therefore, it might be possible that our spectroscopic distance is overestimated. Griggio et al. (2023) find that the proper motions of WD5 are not compatible with those of the cluster. This is consistent with our finding that WD5 is a foreground star. The other white dwarfs (WD4, WD6, and WD7) were not included in the Griggio et al. (2023) study.

Given the current age of M37, the lightest white dwarf members that could have formed through canonical single-star evolution are expected to have masses of  $\approx 0.7 M_{\odot}$  (Griggio et al. 2022). Within the error limits, this is the case for WD1, WD2, WD5, and WD7. However, the mass of WD3 – whose cluster membership is confirmed according to its proper motion – is clearly below  $0.6 M_{\odot}$ . This could be a product of binary evolution, yet it is also possible that our mass is underestimated due to systematic errors in the spectral analysis. The remaining two DAs, WD4 and WD6, have masses of  $0.51 \pm 0.11 M_{\odot}$  and  $0.57 \pm 0.06 M_{\odot}$ , respectively. For WD4, a cluster membership seems unlikely in any case due to its spectroscopic distance. But since the spectroscopic distance of WD6 agrees with that of M37, it seems possible that this star evolved through binary evolution. We note that there is an indication that the binary fraction along the main sequence in M37 is close to 20% (Kalirai & Tosi 2004); thus, it appears plausible that at least some of the white dwarfs in M37 have masses below  $0.7 M_{\odot}$ . In essence, the only DA white dwarf from our sample that is a member of M37 and has a mass consistent with single-star evolution is WD2. Therefore, WD2 can be used to constrain the IFMR, and as such we include it in Fig. 4. As for the central star WD1, its cooling age (0.51 Myr) is negligible in comparison with the cluster age, and thus both WD1 and WD2 had the same initial mass.

**Acknowledgements.** We thank the referee for a constructive report. NR is supported by the Deutsche Forschungsgemeinschaft (DFG) through grants GE2506/17-1 and RE3915/2-1. MG and LRB acknowledge partial support by MIUR under PRIN programme #2017Z2HSMF and by PRIN-INAF2019. MEC acknowledges grant RYC2021-032721-I, funded by MCIN/AEI/10.13039/501100011033 and by the European Union NextGenerationEU/PRTR. PG thanks Marcel Drechsler and Sven Eklund for their contribution to PN imaging. RR acknowledges support from Grant RYC2021-030837-I funded by MCIN/AEI/10.13039/501100011033 and by “European Union NextGenerationEU/PRTR”. This work was partially supported by the AGAUR/Generalitat de Catalunya grant SGR-386/2021 and by the Spanish MINECO grant PID2020-117252GB-I00. The TMAD tool (<http://astro.uni-tuebingen.de/~TMAD>) used for this paper was constructed as part of the activities of the German Astrophysical Virtual Observatory. Based on observations made with the Gran Telescopio Canarias (GTC), installed at the Spanish Observatorio del Roque de los Muchachos of

the Instituto de Astrofísica de Canarias, on the island of La Palma. The Starlink software (Berry et al. 2022) is currently supported by the East Asian Observatory. Some of the data presented in this paper were obtained from the Mikulski Archive for Space Telescopes (MAST). This research has made use of NASA’s Astrophysics Data System and the SIMBAD database, operated at CDS, Strasbourg, France. This research has made use of the VizieR catalogue access tool, CDS, Strasbourg, France. This work has made use of data from the European Space Agency (ESA) mission *Gaia*.

## References

- Alam, S., Albareti, F. D., Allende Prieto, C., et al. 2015, *ApJS*, 219, 12
- Althaus, L. G., Panei, J. A., Miller Bertolami, M. M., et al. 2009, *ApJ*, 704, 1605
- Bailer-Jones, C. A. L., Rybizki, J., Fouesneau, M., Demleitner, M., & Andrae, R. 2021, *AJ*, 161, 147
- Barnett, J. W., Williams, K. A., Bédard, A., & Bolte, M. 2021, *AJ*, 162, 162
- Berry, D., Graves, S., Bell, G. S., et al. 2022, in *Astronomical Society of the Pacific Conference Series*, 532, eds. J. E. Ruiz, F. Pierfederici, & P. Teuben, 559
- Bianchi, L., Shiao, B., & Thilker, D. 2017, *ApJS*, 230, 24
- Bressan, A., Marigo, P., Girardi, L., et al. 2012, *MNRAS*, 427, 127
- Chambers, K. C., Magnier, E. A., Metcalfe, N., et al. 2016, arXiv e-prints [arXiv:1612.05560]
- Chang, S. W., Byun, Y. I., & Hartman, J. D. 2015, *AJ*, 150, 27
- Chornay, N., & Walton, N. A. 2020, *A&A*, 638, A103
- Cummings, J. D., Kalirai, J. S., Tremblay, P. E., & Ramirez-Ruiz, E. 2015, *ApJ*, 807, 90
- Cummings, J. D., Kalirai, J. S., Tremblay, P. E., Ramirez-Ruiz, E., & Bergeron, P. 2016, *ApJ*, 820, L18
- Cummings, J. D., Kalirai, J. S., Tremblay, P. E., Ramirez-Ruiz, E., & Choi, J. 2018, *ApJ*, 866, 21
- Drew, J. E., Greimel, R., Irwin, M. J., et al. 2005, *MNRAS*, 362, 753
- Fitzpatrick, E. L., Massa, D., Gordon, K. D., Bohlin, R., & Clayton, G. C. 2019, *ApJ*, 886, 108
- Fragkou, V., Parker, Q. A., Zijlstra, A., Shaw, R., & Lykou, F. 2019, *MNRAS*, 484, 3078
- Fragkou, V., Parker, Q. A., Zijlstra, A. A., et al. 2022a, *Galaxies*, 10, 44
- Fragkou, V., Parker, Q. A., Zijlstra, A. A., et al. 2022b, *ApJ*, 935, L35
- Gaia Collaboration (Brown, A. G. A., et al.) 2021, *A&A*, 649, A1
- Griggio, M., & Bedin, L. R. 2022, *MNRAS*, 511, 4702
- Griggio, M., Bedin, L. R., Raddi, R., et al. 2022, *MNRAS*, 515, 1841
- Griggio, M., Salaris, M., Nardiello, D., et al. 2023, *MNRAS*, 524, 108
- Hall, P. D., Tout, C. A., Izzard, R. G., & Keller, D. 2013, *MNRAS*, 435, 2048
- Horne, K. 1986, *PASP*, 98, 609
- Hügelmeier, S. D., Dreizler, S., Homeier, D., et al. 2006, *A&A*, 454, 617
- Kalirai, J. S., & Tosi, M. 2004, *MNRAS*, 351, 649
- Kalirai, J. S., Richer, H. B., Reitzel, D., et al. 2005, *ApJ*, 618, L123
- Kepler, S. O., Pelisoli, I., Koester, D., et al. 2016, *MNRAS*, 455, 3413
- Koester, D. 2010, *Mem. Soc. Astron. Italiana*, 81, 921
- Marsh, T. R. 1989, *PASP*, 101, 1032
- Miller Bertolami, M. M. 2016, *A&A*, 588, A25
- Monguió, M., Greimel, R., Drew, J. E., et al. 2020, *A&A*, 638, A18
- Napiwotzki, R. 1999, *A&A*, 350, 101
- Page, M. J., Brindle, C., Talavera, A., et al. 2012, *MNRAS*, 426, 903
- Parker, Q. A., Frew, D. J., Miszalski, B., et al. 2011, *MNRAS*, 413, 1835
- Reindl, N., Bainbridge, M., Przybilla, N., et al. 2019, *MNRAS*, 482, L93
- Reindl, N., Schaffenroth, V., Filiz, S., et al. 2021, *A&A*, 647, A184
- Reindl, N., Islami, R., Werner, K., et al. 2023, *A&A*, 677, A29
- Renedo, I., Althaus, L. G., Miller Bertolami, M. M., et al. 2010, *ApJ*, 717, 183
- Sabin, L. 2008, PhD thesis, University of Manchester
- Unglaub, K., & Bues, I. 2000, *A&A*, 359, 1042
- Werner, K. 1992, in *The Atmospheres of Early-Type Stars*, 401, eds. U. Heber & C. S. Jeffery, 273
- Werner, K., & Herwig, F. 2006, *PASP*, 118, 183
- Werner, K., Dreizler, S., Heber, U., et al. 1995, *A&A*, 293, L75
- Werner, K., Deetjen, J. L., Dreizler, S., et al. 2003, in *Stellar Atmosphere Modeling*, eds. I. Hubeny, D. Mihalas, & K. Werner, *Astronomical Society of the Pacific Conference Series*, 288, 31
- Werner, K., Rauch, T., & Kepler, S. O. 2014, *A&A*, 564, A53
- Werner, K., Rauch, T., & Kruk, J. W. 2018, *A&A*, 609, A107
- Werner, K., Rauch, T., & Reindl, N. 2019, *MNRAS*, 483, 5291
- Werner, K., Reindl, N., Geier, S., & Pritzkeleit, M. 2022, *MNRAS*, 511, L66